Model-Based Maximum Power Point Tracking for Photovoltaic Panels: Parameters Identification and Training Database Collection

Loredana Cristaldi, Marco Faifer, Christian Laurano, Roberto Ottoboni, Sergio Toscani, Michele Zanoni

DEIB, Politecnico di Milano, Piazza Leonardo da Vinci 32, 20133 Milano (Italy)
sergio.toscani@polimi.it

Abstract: Module-level distributed maximum power point tracking (DMPPT) represents an attractive solution for photovoltaic systems installed in dense urban areas, where panels are often subject to different solar irradiance levels. Model-based (MB) MPPT algorithms are particularly suitable for the purpose: they enable good steady-state accuracy and fast dynamics thanks to an underlying parametric model of the panel. The target of the present paper is deeply investigating the estimation of the model parameters, and the collection of the training database, since they heavily affect overall performance. In this work, parameter values results by maximizing energy production considering the training database; under some simplifications, it leads to a weighted least squares problem that can be easily solved. One of the main advantages is the robustness in the presence of identification data which have been collected under partially shadowed conditions. Moreover, the possibility to gather the training database by running a perturb and observe MPPT is investigated and tested for the first time. Energy production is allowed also during this stage, thus opening the way to a periodic update of the parameters in order to follow degradation and time drift of the module. Experimental results show that performance is virtually the same as that obtained by computing parameters from a large set of volt-ampere characteristics.

1. Introduction

The last two decades have been characterized by an increasing awareness about the impact of pollution and global warming, and their potentially catastrophic consequences on agriculture, human health, water supply and economy. The vast majority of the scientists agree that the ongoing climate change is mostly caused by anthropogenic greenhouse gas emissions, such as carbon dioxide. Governments and intergovernmental organizations committed to reduce these emissions, also through financial incentive policies.

As far as electricity production, we have experienced a huge increase of the impact of generation from renewable energy sources. Among them, photovoltaic (PV) systems have played a primary role [1]. The main reason is their modularity: they can be easily installed and scaled up from residential applications to multi-MW solar parks. In order to quantify their proliferation, on April 20th 2020, 40% of electricity production in Germany was solar-generated [2], an impressive figure especially when compared to the 22% provided by coal and nuclear plants during the same day [3].

A major drawback of PV systems is their low conversion ratio, which is below 20% [4] mostly because of the poor efficiency of PV modules (or panels). Optimizing energy production and cost effectiveness is mandatory especially in the present scenario, since governments have generally reduced their incentives [5]. However, a major role in overall efficiency is also played by the power electronics converters which are required in order to interface the modules with the ac grid. In particular, they allow setting the operating point on the volt-ampere characteristics of the panels in order to maximize power output for given environmental conditions (mostly temperature and solar irradiance level) thanks to a maximum power point tracking (MPPT) algorithm. Because of its importance, it is not surprising that this topic is widely studied in order to balance out simplicity, steady-state accuracy and dynamic performance, namely the capability to follow the maximum power point (MPP) even during the fast variations of the irradiance level which may occur. The simplest MPPT techniques, which are still largely employed, include fractional open circuit voltage, perturb and observe (P&O) [6] and incremental conductance method [7]. These two last techniques are extremely similar [8], and they approach the MPP by periodically applying a positive or negative voltage perturbation to the modules; increasing its magnitude leads to faster dynamics at the expense of a wider oscillation around the MPP once it has been reached. In order to overcome this issue, adaptive step algorithms have been proposed [9], [10]. Many different MPPT techniques and implementations can be found in the literature [11]-[14], for example based on sliding mode control [15], [16], fuzzy logic [17], [18], model predictive control [19], artificial neural networks [20] as well as several other approaches.

Grid-tied PV systems are typically made of strings of series-connected PV modules; one or more strings (thus composing a PV array) feed a dc/dc or a dc/ac converter. Assuming that all the modules are identical and the solar irradiance on the panels is uniform, the power-voltage curve of the array shows a clearly identifiable MPP and (theoretically) no other inflection points. Unfortunately, in practical applications the curve may exhibit local maxima: PV panels have some degree of mismatch between their electrical characteristic, and, most important, they may be subject to different irradiance levels. In this case, the employed MPPT algorithm may converge to a local maximum without reaching the MPP, thus resulting in a significant decrease of energy production [21]. In the literature several MPPT techniques have been specifically developed to deal with this issue [22]-[25]. However, it is worth noting that even if the string or array is working at its global MPP, output may be significantly lower with respect to that achieved if all the modules were operating at their individual MPPs. Studies show that in a real-world scenario, this loss may be between 3 and 16% in case of nonuniform irradiance on the panels [26].

The problem of mismatched operating conditions over the

different panels is exacerbated by the proliferation of small-scale, urban PV installations. Modules are often subject to different irradiance levels, either because of shadowing due to the complex landscapes in cities, or different orientations. In order to optimize energy production under these conditions, many authors have proposed to implement distributed maximum power point tracking (DMPPT) by dividing the PV array into sub-sections [27], [28]. In this respect, module-level DMPPT is becoming attractive, and it can be enabled thanks to the employment of microinverters [29], [30] or module-integrated dc-dc converters [31]-[33]. Some works investigated also subpanel [34] and cell-level DMPPT, but the inherent cost and complexity hardly make it as viable options for commercial applications in a near future [26].

In principle, the same algorithms employed for the conventional, string-level MPPT could be adopted also to implement module-level DMPPT. However, the electrical behavior of a single PV panel can be accurately represented with simple parametric models receiving cell temperature and irradiance level as inputs [35], [36], which are assumed to be uniform over the module itself. For this reason, different MPPT techniques based on a model of the PV panel have been proposed in the literature. The underlying model allows predicting the location of the MPP for given environmental conditions, and this result in good steady state accuracy and, in particular, exemplary dynamic performance. In general, these techniques require measuring both the panel temperature and the solar irradiance level [37], [38]: unfortunately this needs an expensive radiation sensor for each module, or few modules. In some cases, solar radiation is indirectly obtained from the short circuit current of the module [39].

In order to overcome this limitation, the authors of the present work have studied a model-based (MB) MPPT algorithm that requires measuring the solar radiation only during the estimation of the model parameters, but not during regular operation [40], [41]. Furthermore, [42] proposes an innovative, iterative MB-MPPT method that allows completely avoiding the measurement of solar radiation level; comparison with other, well-known algorithms show the effectiveness of the approach [43]. As for the other MB techniques, it requires a preliminary identification of the parameters before it can be put in operation. This stage has vital importance, since the quality of the parameters estimates directly affects performance. Identification data is represented by a proper set of volt-ampere curves, which should be measured under different environmental conditions according to the assumptions of the underlying model. During the collection of the training dataset, energy production is interrupted. Parameter estimates are obtained with the least squares approach, namely minimizing the mean squared error of the predicted MPP voltage.

The target of the present paper is deeply investigating and improving the model identification process, in order to achieve maximum efficiency. In this work, parameters are obtained as the result of an optimization problem, aimed at maximizing energy production considering the identification dataset. Having introduced proper approximations, the solution corresponds to a weighted least squares estimate having a closed-form expression [44]. Performances will be compared to those achieved by using parameters obtained with the conventional method. Experimental results highlight the robustness of the new approach with respect to identification data collected under partial shadowing, as it may happen in practical applications.

For the first time this article scouts the possibility to estimate model parameters from data collected during the execution of a simple P&O MPPT algorithm with a coarse voltage perturbation step. In this way, energy is delivered to the grid even during the training stage, and thus it opens the way to a periodic retuning of the parameters in order to follow aging and time-drifts of the PV modules. Experimental results show that efficiency is on par with that obtained as long as parameters are computed using the volt-ampere curves.

2. Iterative Model Based MPPT algorithm

Let us consider a PV panel connected to its own power electronics converter which permits controlling the output voltage; this enables the implementation of module-level DMPPT. For the purpose, [42] proposes an iterative MB-MPPT algorithm that allows avoiding a direct measurement of solar irradiance. The target is having available an estimate of the MPP voltage V_{MP} which, in turn, can be used as the reference value V_{ref} for the module voltage controller. The approach starts from a well-known analytical expression [45] that allows obtaining V_{MP} as a two-variable function of the module temperature T_p and of the solar radiation G, assumed to be uniform over the panel. After some approximations and manipulations, it is possible to write:

$$V_{ref} = V_{MP} \simeq A_0 + A_1 T_p + A_2 \ln\left(I_{MP}\right) + A_3 \ln^2\left(I_{MP}\right) \quad (1)$$

where I_{MP} is the module current at MPP while $A_0 \div A_3$ are parameters depending on the behavior of the specific panel. Of course, this expression cannot be directly employed in order to obtain V_{MP}: while T_p can be easily measured, I_{MP} is unknown. Therefore, let us substitute I_{MP} with I_m, which is the measured module current in the operating point:

$$V_{ref} = A_0 + A_1 T_p + A_2 \ln\left(I_m\right) + A_3 \ln^2\left(I_m\right) \quad (2)$$

of course, since I_m is in general different from I_{MP}, the reference voltage V_{ref} of the controller is not equal to V_{MP}. However, if V_{ref} is updated iteratively using (2) with the new measured current I_m (converter and module dynamics is neglected) and module temperature T_p, it rapidly converges in the neighborhood of V_{MP}. During the first iteration a measurement of the module current is not available. In this case, V_{ref} is initially set to:

$$V_{ref} = A_0 + A_1 T_p \quad (3)$$

2.1. Model identification

MB-MPPT algorithms operate thanks to *a priori* knowledge about the behavior of the panel, which is represented by a proper model. The adopted approach which has been discussed in the previous section is based on a four-parameter model expressed by (1); before starting the operation, $A_0 \div A_3$ have to be properly estimated during a preliminary training stage. It is worth noting that (1) is linear in the parameters: I_m and T_p are known, thus V_{ref} is a linear combination of $A_0 \div A_3$. Let us suppose having available a

database made of N observations of panel current and voltage at MPP together with the corresponding temperature, which have been collected under different environmental conditions. The generic nth observation is characterized by the triplet of values $V_{MP}^{[n]}$, $I_{MP}^{[n]}$, $T_p^{[n]}$. Assuming that (1) holds true, the following system of equations can be written using the matrix notation:

$$\begin{bmatrix} V_{MP}^{[1]} \\ V_{MP}^{[2]} \\ \vdots \\ V_{MP}^{[N]} \end{bmatrix} = \begin{bmatrix} 1 & T_p^{[1]} & \ln\left(I_{MP}^{[1]}\right) & \ln^2\left(I_{MP}^{[1]}\right) \\ 1 & T_p^{[2]} & \ln\left(I_{MP}^{[2]}\right) & \ln^2\left(I_{MP}^{[2]}\right) \\ \vdots & \vdots & \vdots & \vdots \\ 1 & T_p^{[N]} & \ln\left(I_{MP}^{[N]}\right) & \ln^2\left(I_{MP}^{[N]}\right) \end{bmatrix} \begin{bmatrix} A_0 \\ A_1 \\ A_2 \\ A_3 \end{bmatrix} \quad (4)$$

$$\mathbf{V}_{MP} = \mathbf{F}\mathbf{A}$$

Now the target is evaluating the model parameters which are the components of the column vector **A**. Assuming that matrix **F** has full column rank, (4) represents an overdetermined system of equations. Under this assumption, an estimate $\mathbf{A}_{LS}$ of **A** can be obtained by using the Moore-Penrose inverse of **F**:

$$\mathbf{A}_{LS} = \left(\mathbf{F}^T\mathbf{F}\right)^{-1}\mathbf{F}^T\mathbf{V}_{MP} \quad (5)$$

^{T} indicates matrix transpose operator and $\mathbf{A}_{LS}$ represents the least-squares (LS) estimate of **A**, which is the solution of the unconstrained minimization problem:

$$\arg\min_{\mathbf{A}} \left\|\mathbf{V}_{MP} - \mathbf{F}\mathbf{A}\right\| \quad (6)$$

where $\|\ \|$ denotes the L^2 (or Euclidean) norm. Therefore $\mathbf{A}_{LS}$ contains the model parameter estimates that minimize a cost function represented by the L^2 norm of the vector containing the deviations between the N measured MPP voltages and the corresponding model predictions. However, this cost function is not directly connected with the goal of a MB-MPPT, which is maximizing energy production for given environmental conditions. Instead, this correspond to the minimization of a different cost function Φ: for a given time interval $[t_0, t_1]$ it is defined as the difference between the energy E_{MP} produced by ideally tracking the actual MPP, and E_e, namely that generated by operating at the maximum power point voltages predicted by the model:

$$\Phi = E_{MP} - E_e \quad (7)$$

Φ can be easily rewritten in terms of power. For the purpose, let us introduce $P(V,t)$ as the power-voltage characteristics of the module corresponding to the environmental conditions in the time instant t and $P_{MP}(t)$ as the generated power at the MPP in the same instant. It results:

$$\Phi = \int_{t_0}^{t_1}\left[P_{MP}(t) - P\left(V_{MP,e}(\mathbf{A},t),t\right)\right]dt \quad (8)$$

where $V_{MP,e}(\mathbf{A},t)$ is the MPP voltage in the time instant t predicted by the model (1) defined by the parameter vector **A**. As aforementioned, an estimate of **A** can be obtained from the minimization of Φ, but a continuous-time expression as (8) is obviously not suitable for practical applications. Let us suppose that the N observations in the training database refer to evenly-spaced time instants over the considered interval $[t_0, t_1]$. Under this assumption, a discretized expression of Φ can be easily derived; therefore model parameters can be obtained by solving:

$$\arg\min_{\mathbf{A}} \sum_{n=1}^{N}\left[P_{MP}^{[n]} - P^{[n]}\left(\mathbf{F}^{[n]}\mathbf{A}\right)\right] \quad (9)$$

where $\mathbf{F}^{[n]}$ is the nth row of matrix **F**, while $P_{MP}^{[n]}=V_{MP}^{[n]}I_{MP}^{[n]}$. However, the estimation problem is still troublesome, since it contains $P^{[n]}(V)$, which is the power-voltage curve of the module corresponding to the nth observation. The predicted MPP voltage is hopefully rather close to the actual value: in this respect, a second order approximation of $P^{[n]}(V)$ in the neighborhood of the actual MPP voltage $V_{MP}^{[n]}$ can be employed. Reminding that by definition its first-order derivative is zero at $V_{MP}^{[n]}$, the previous approximation leads to:

$$P\left(\mathbf{F}^{[n]}\mathbf{A}\right) \simeq P_{MP}^{[n]} - W^{[n]}\left(\mathbf{F}^{[n]}\mathbf{A} - V_{MP}^{[n]}\right)^2 \quad (10)$$

where:

$$W^{[n]} = -\frac{1}{2}\frac{d^2P^{[n]}(V)}{dV^2}\bigg|_{V_{MP}^{[n]}} \quad (11)$$

Using (10) into (9) leads to a different formulation of the optimization problem to be solved:

$$\arg\min_{\mathbf{A}} \sum_{n=1}^{N} W^{[n]}\left(\mathbf{F}^{[n]}\mathbf{A} - V_{MP}^{[n]}\right)^2 \quad (12)$$

Let us introduce **W** as an $N\times N$ diagonal matrix whose nth diagonal entry is $W^{[n]}$:

$$\mathbf{W} = \begin{bmatrix} W^{[1]} & 0 & \dots & 0 \\ 0 & W^{[2]} & \vdots & \vdots \\ \vdots & \vdots & \ddots & 0 \\ 0 & 0 & \dots & W^{[N]} \end{bmatrix} \quad (13)$$

Using matrix notation (12) can be rewritten as:

$$\arg\min_{\mathbf{A}} \left\|\mathbf{W}^{1/2}\left(\mathbf{V}_{MP} - \mathbf{F}\mathbf{A}\right)\right\| \quad (14)$$

The corresponding solution $\mathbf{A}_{WLS}$ is the weighted least squares (WLS) estimate of the model coefficients using **W** as the weighting matrix. Now the problem is obtaining the diagonal entries $W^{[n]}$ of matrix **W**. Assuming that for the generic nth observation the curve $P^{[n]}(V)$ have been acquired, $W^{[n]}$ can be estimated by means of a local polynomial fitting of the curve in the neighborhood of $V_{MP}^{[n]}$. The clear drawback of this solution is that additional data have to be measured, stored and processed, thus the complexity of the identification procedure increases significantly.

An alternative solution starts from the observation that the second-order derivative of the curve $P(V)$ around V_{MP} is approximatively proportional to P_{MP} [44]. Thanks to this observation, reminding that the WLS solution is not affected by scaling the weight matrix, **W** can be substituted in (14) with another $N\times N$ diagonal matrix $\mathbf{P}_{MP}$ whose nth diagonal entry corresponds to $P_{MP}^{[n]}$.

$$\mathbf{P}_{MP} = \begin{bmatrix} P_{MP}^{[1]} & 0 & \dots & 0 \\ 0 & P_{MP}^{[2]} & \vdots & \vdots \\ \vdots & \vdots & \ddots & 0 \\ 0 & 0 & \dots & P_{MP}^{[N]} \end{bmatrix} \quad (15)$$

Therefore, the WLS estimate of **A** results:

$$\mathbf{A}_{WLS} = \left(\mathbf{F}^T\mathbf{P}_{MP}\mathbf{F}\right)^{-1}\mathbf{F}^T\mathbf{P}_{MP}\mathbf{V}_{MP} \quad (16)$$

Thanks to this simplification, computing the WLS solution requires the same identification data as the LS estimate. In particular, it is no longer necessary to acquire and store the $P(V)$ curve for each training point, but only the MPP voltage, current and the corresponding panel temperature.

2.2. Database Collection

According to the previous considerations, computing the model parameters requires N triplets of measured MPP voltage, current and module temperature (that is $V_{MP}^{[n]}, I_{MP}^{[n]}, T_p^{[n]}$, $n \in \{1,\ldots,N\}$) collected under different environmental conditions and resulting in a full-column rank matrix $\mathbf{F}$. It is evident that the quality of the training data may significantly affect the estimated parameters and thus the performance of the MB-MPPT algorithm. For best results, model parameters should be identified by using a training dataset that somehow includes the environmental conditions which may occur during typical operation. Furthermore, data should be collected according to the underlying assumptions of the model, e.g. solar radiation is assumed to be uniform over the panel.

A first possibility to gather these data is collecting N volt-ampere characteristics of the module and measuring the corresponding temperatures. From each curve, the maximum power point voltage and current can be accurately extracted by means of proper techniques. This approach, which is the most intuitive choice also adopted in previous papers [40]-[44], suffers from several limitations. First of all, it requires hardware having this capability, but most important, the panel cannot produce deliver energy to the grid when training data is collected.

An attractive alternative is building the database by operating the module with a simple MPPT technique which does not require a knowledge base, thus enabling energy production even during this stage. The reached operating points are periodically stored in the database.

The well-known P&O algorithm [6] can be favorably adopted for the purpose. Basically a voltage perturbation ΔV is applied to the module voltage and the corresponding variation ΔP of the power output is measured. If ΔP is positive, it means that the module voltage is moving towards the MPP, thus in the next sampling instant another voltage perturbation having the same sign as before is superimposed. Otherwise, if ΔP is negative, the sign of the voltage perturbation is reversed, since it indicates that the previous perturbation was bringing the module voltage away from the MPP. Under steady-state conditions, the module voltage oscillates around the MPP voltage; the amplitude of this oscillation corresponds to the amplitude of the voltage perturbation. A critical aspect of the P&O method is selecting the magnitude of the voltage perturbation. In particular, a large voltage perturbation allows effective tracking rapidly changing conditions, but the steady state efficiency is jeopardized. Conversely, a small voltage perturbation trades dynamic performance for steady-state accuracy; furthermore, it becomes more sensitive with respect to measurement noise.

When the database is collected by running the P&O algorithm, MPP current and voltage are unavoidably affected by the perturbation step, which acts similarly to an additive noise contribution. The resulting performance degradation must be assessed. Furthermore, having not available the shape of the volt-ampere curve, it becomes more difficult to recognize (and possibly discard) identification data that have not been collected according to the model assumptions, in particular during partially shaded conditions. Therefore, the parameter estimation algorithm should be robust with respect to this somewhat corrupted data.

3. Experimental Setup

The first target is comparing the performance which can be achieved by the iterative MB-MPPT algorithm when parameters are estimated by using either the LS or the WLS approach. After that, it will be quantified the additional loss which occurs as long as the training dataset is obtained by running a P&O MPPT algorithm instead of acquiring the whole volt-ampere curves.

A commercial PV module made of 72 125 mm × 125 mm mono crystalline silicon cells has been employed. Rated power is 180 W under standard test conditions (1000 W/m^2 solar radiation intensity, 25°C cell temperature, 1.5 air mass coefficient), which is reduced to 130 W when considering nominal operating cell temperature and 800 W/m^2 irradiance level. Nominal short circuit current is I_{sc}=5 A, while open circuit voltage is V_{oc}=40 V. The panel has been connected to a test system that allows controlling its operating point on the V-I characteristics while performing the required measurements. Part of it is located on the roof of the building, part in our lab. Since it is not possible to take a comprehensive picture of the setup, its architecture is depicted in Fig. 1 for the sake of clarity

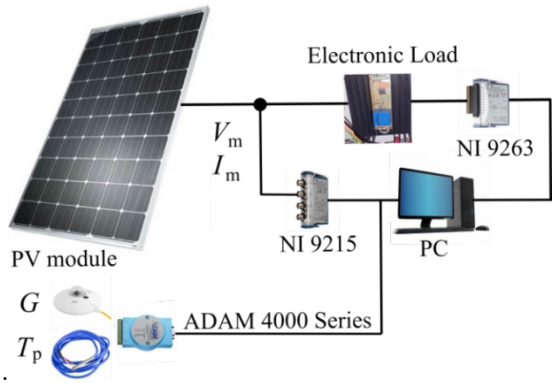

Fig. 1. Experimental setup

Panel temperature and solar radiation have been monitored by means of a Pt100 and a Kipp & Zonen CMP21 class A pyranometer which have been connected to the PC installed in our lab by using Advantec ADAM 4000 series sensor interfaces. The output terminals of the module are connected to a custom-built linear electronic load, located in the lab, which allows controlling the voltage according to a reference value V_{ref}. The panel voltage is scaled down thanks to a resistive divider in order to be properly acquired, while a closed-loop Hall effect sensor (LEM LA25NP connected in order to have 5 A nominal current) allows current measurement. The reference voltage for the electronic load is provided by a National Instruments NI-9263, 16 bit 100 kS/s voltage output module. Panel voltage and current signals have

been acquired with a National Instruments NI-9215 voltage input module having simultaneous sampling capability, 16-bit resolution and 100 kS/s maxim rate per channel. The measurement process and the control of the electronic load have been managed by a PC running a proper LabView Virtual Instrument. A picture of the setup is reported in Fig. 2: it is conceived to monitor up to 4 PV modules simultaneously, so it comprises 4 electronic loads and an adequate number of analog input channels in order to monitor their currents and voltages. Of course, only the leftmost electronic load has been employed for the purpose of this work.

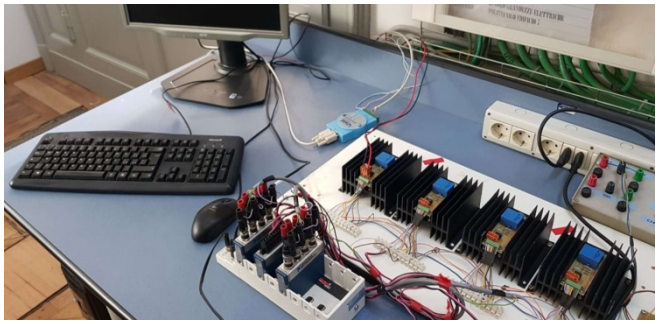

Fig. 2. Electronic load and data acquisition system

The previously described experimental setup allows acquiring the volt-ampere characteristics of the module by imposing a proper voltage ramp as the reference voltage for the electronic load. 100 ms ramp-up time and 100 kHz sampling rate have been employed. Solar radiation and temperature can be considered as constant during this short time interval. Every minute, 10 *V-I* curves have been recorded (the operation takes about 1 s) together with the corresponding module temperature and solar irradiance level.

4. Experimental Results

Data acquisition has been performed during a clear, sunny day and $N = 490$ blocks of 10 volt-ampere curves have been acquired. The generic nth block (n=1…N) is characterized by a corresponding value of panel temperature $T_p^{[n]}$ and solar irradiance level $G^{[n]}$, which has been saved for monitoring purposes but it is not required by the considered algorithms. Voltage and current waveforms have been processed with proper FIR filters in order to reduce the impact of measurement noise. These filters have been specifically designed in order to preserve the shape of the acquired *V-I* characteristics. After filtering, considering the last filtered *V-I* curve of each nth block, the corresponding *P-V* characteristics has been computed. The MPP has been accurately located by means of a smoothing spline; the maximum power value $P_{MP}^{[n]}$ and the corresponding voltage and current values ($V_{MP}^{[n]}$ and $I_{MP}^{[n]}$, respectively) are easily obtained. $P_{MP}^{[n]}$ is the theoretical maximum power that can be produced under given conditions, achieved by an ideal MPPT: therefore it represents the performance benchmark for MPPT algorithms. Fig. 3 reports its time evolution over the considered day, together with the solar irradiance level.

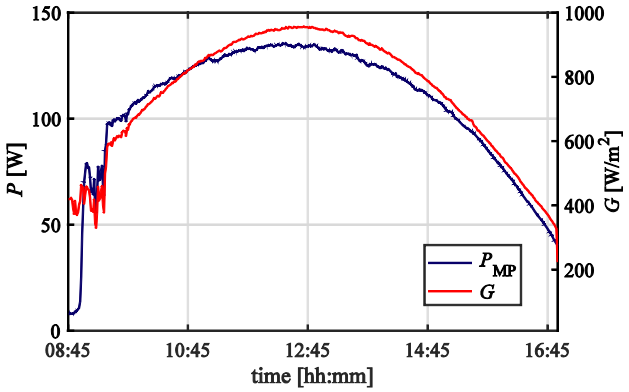

Fig. 3. Trend of maximum power and of the corresponding solar irradiance level

The plot of the maximum power exhibits a jagged trend in the leftmost part: it is due to partial shadowing caused by a nearby building.

4.1. Impact of the estimator and partial shadowing

Having available N triplets of values $V_{MP}^{[n]}$, $I_{MP}^{[n]}$ and $T_p^{[n]}$ which have been obtained from experimental data as discussed in the previous subsection, the model parameters of the MB-MPPT algorithm can be estimated with either the LS and the WLS approach. The obtained values for $A_0 \div A_3$ are reported in TABLE I. It can be clearly noticed that numerical values resulting from the two estimators exhibit significant differences.

TABLE I
ESTIMATED PARAMETERS

Estimator	A_0 [V]	A_1 [V K^{-1}]	A_2 [V]	A_3 [V]
LS	36.105	-0.0673	-1.24	-0.921
WLS	37.281	-0.124	-0.699	-1.22

After that, the collected curves have been employed to run the iterative MB-MPPT algorithm with the parameters obtained with both of the approaches. In particular, the ten curves of each block have been used to emulate the execution of the algorithm, as if it were running with a 100 ms time step. For the generic nth block, the module voltage reached by the algorithm in the last curve is $V_a^{[n]}$ (that is the predicted MPP voltage), while $P_a^{[n]}$ represents the corresponding power output. Ideally, $V_a^{[n]}$ should be $V_{MP}^{[n]}$ so that $P_a^{[n]}$ should be equal to $P_{MP}^{[n]}$; of course $P_a^{[n]} \leq P_{MP}^{[n]}$. The initial module voltage has been set as that reached at the end of the previous block.

First of all, the target is comparing the tracking capabilities of the MB-MPPT algorithm when the parameters have been obtained with the LS and WLS estimator. For the purpose, the absolute value of the difference between the actual and predicted MPP voltages has been computed in each block:

$$\Delta V_{MP}^{[n]} = \left| V_a^{[n]} - V_{MP}^{[n]} \right| \qquad (17)$$

Fig. 4 reports the achieved results.

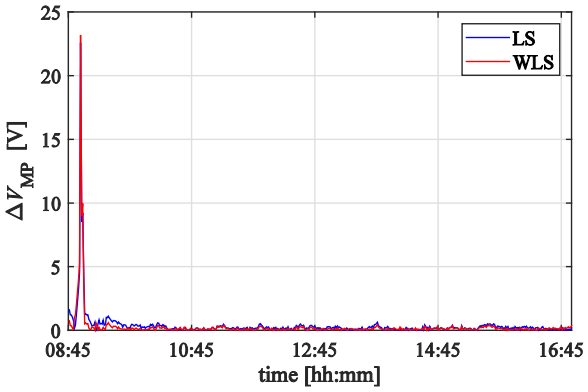

Fig. 4. Difference between actual and predicted MPP voltage: parameters estimated with LS and WLS approach

A significant peak can be immediately noticed just before 9 am; here, the difference between the MPP voltage predicted by the algorithms and the actual one is extremely large, exceeding 20 V with respect to the 40 V rated open circuit voltage. When comparing Fig. 3 to Fig. 4, it becomes evident that this peak occurs because of partial shadowing. Some of the volt-ampere characteristics which have been collected under these conditions are reported in Fig. 5, while the corresponding $P(V)$ curves are shown Fig. 6.

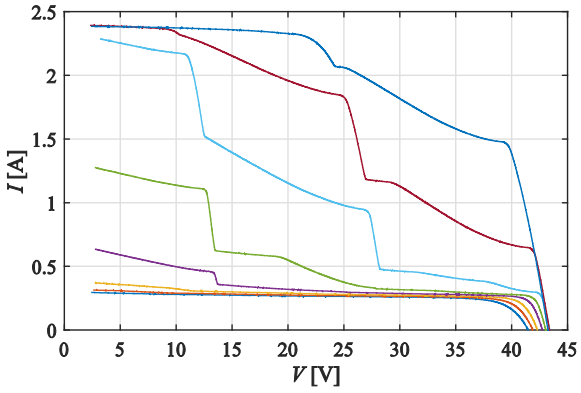

Fig. 5. V-I curves acquired under partial shadowing

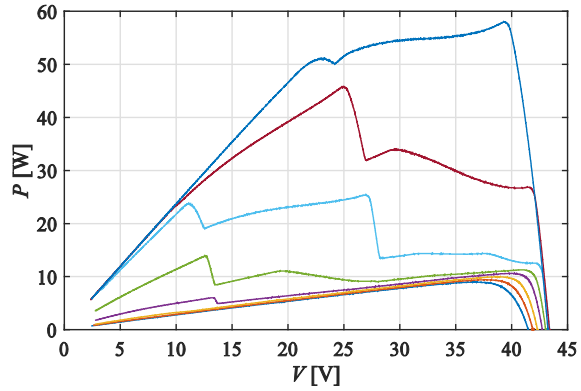

Fig. 6. P-V curves acquired under partial shadowing

Multiple local maxima are clearly noticeable in in the $P(V)$ characteristics: the assumptions which the MB-MPPT algorithm is based on are not met; therefore weak performance is expected in this case.

Now, let us focus on the part of the day when partial shading is much less severe, thus after 9 am. In particular, Fig. 7 compares the actual MPP voltages with those reached by the MB-MPPT algorithm using either the parameters estimated with the LS or the WLS approach. It can be noticed that the if the parameters are obtained with the WLS estimator, the MB-MPPT algorithm allows a better tracking of the MPP voltage, either at the beginning and in the middle part of the day, thus when solar irradiance level is maximum and hence also power output. In the final part of the day, using the parameters obtained with the LS or WLS approach leads to similar results.

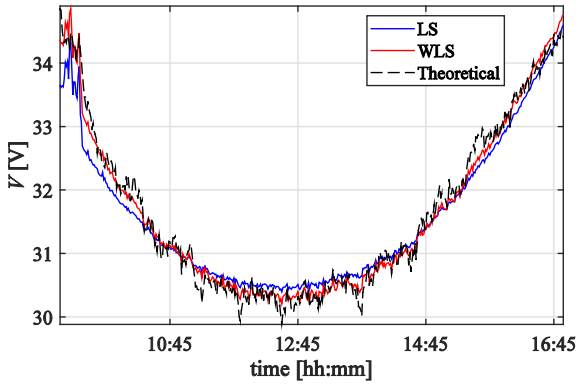

Fig. 7. Comparison between predicted and theoretical MPP voltage: parameters estimated with LS and WLS approach

Accurate tracking of the MPP voltage is not the final goal for a MPPT algorithm: on the contrary, it is maximizing energy production during a typical day. In this respect, a very significant performance indicator is represented by the cumulative energy loss with respect to ideal conditions (operation always perfectly tied to the actual MPP, thus power output equal to P_{MP}). Assuming constant environmental conditions between two blocks of curves, the cumulative energy loss $\Delta E_e^{[n]}$ can be simply computed as:

$$\Delta E_e^{[n]} = \sum_{i=1}^{n} \left(P_{MP}^{[i]} - P_a^{[i]} \right) \Delta t \qquad (18)$$

where Δt is the time interval occurring between the acquisition of two blocks of 10 characteristics (namely 60 s). Using (18), the expression of $\Delta E_{e,r}$, that is the cumulative energy loss in relative value, can be obtained as:

$$\Delta E_{e,r}^{[n]} = 1 - \frac{\sum_{i=1}^{n} P_a^{[i]}}{\sum_{i=1}^{n} P_{MP}^{[i]}} \qquad (19)$$

The better performance achieved as long as the parameters are estimated with the WLS approach is immediately evident from Fig. 8: at the beginning of the day, losses are about 0.3%, while they exceed 1% if the parameters are obtained with the LS estimator.

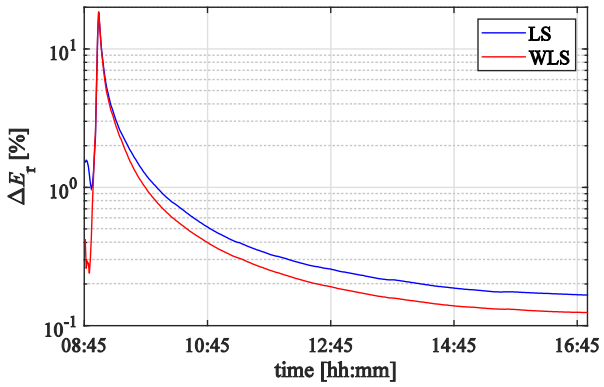

Fig. 8. Cumulative energy loss in relative value: parameters estimated with LS and WLS approach

In case of severe partial shadowing, performance is poor in both cases, since relative loss approaches 20%. Once we move away from partial shadowing conditions, as expected relative loss decreases, and once again the MB-MPPT algorithm with parameters obtained by adopting the WLS estimator achieves higher efficiency. At the end of the day, using the WLS estimates results in 0.12% total energy loss, which is about one third lower with respect to that obtained when parameters are computed with the LS estimator (0.17%).

As pointed out during the introduction, partial shadowing has a detrimental effect on PV energy production, with significant decrease of overall efficiency. Furthermore, when computing the parameters of the MB-MPPT using a training database that includes operating conditions which do not comply with the assumption of the model (such as under partial shadowing), the quality of the estimates may degrade. Therefore, it would be interesting to have available a simple method to detect and discard these data.

A simple solution starts from the observation that data collected under partial shadowing are characterized by MPP voltages which are considerably different with respect to those predicted by the model (1) using MPP currents and panel temperatures. Therefore, model parameters have been initially estimated from the whole database. After that, the differences between actual and predicted MPP voltage have been computed. When this difference exceeds in magnitude a threshold value (e.g. 1.5 V) the corresponding data is flagged as outlier and thus removed from the identification set. Finally, parameters have been estimated on the refined database. TABLE II reports the new values of $A_0 \div A_3$ computed with both the LS and WLS approach.

TABLE II
ESTIMATED PARAMETERS, TRAINING DATA UNDER PARTIALLY SHADED CONDITIONS HAVE BEEN DISCARDED

Estimator	A_0 [V]	A_1 [V K^{-1}]	A_2 [V]	A_3 [V]
LS	36.688	-0.146	-0.588	-1.22
WLS	37.600	-0.143	-0.488	-1.36

When comparing TABLE I with TABLE II, it is worth noting that the WLS estimates are rather similar in both cases. On the contrary, parameters obtained by adopting the LS approach are more heavily affected by the presence of training data which have been collected under partial shadowing. Furthermore, when training data obtained in partially shaded conditions is discarded, parameters computed with the LS approach becomes much closer with respect to those obtained with the WLS estimator.

Once again, let us consider these new estimates of the parameters and let us evaluate the performances achieved by the iterative MB-MPPT algorithm in this case. Of course partial shadowing conditions have to be included as long as energy production is evaluated. Cumulative energy loss have been computed and compared, in relative value, with those obtained with the previous parameters (Fig. 8). Results are reported in Fig. 9.

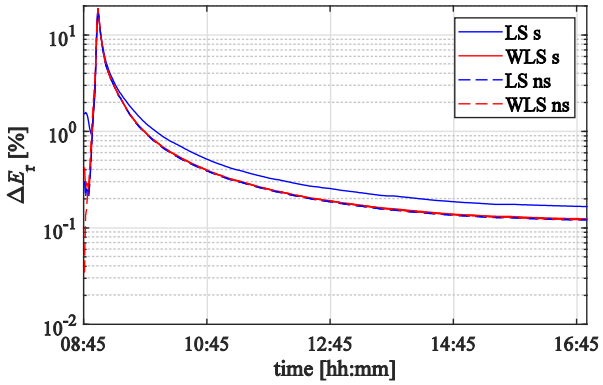

Fig. 9. Relative cumulative energy loss, parameters estimated with LS and WLS approach. Training data include (continuous lines) or discard (dashed lines) points acquired under partially shaded conditions

The most significant result is that, once having removed the data collected under partial shadowing, the efficiency reached by the MB-MPPT is very similar when either the LS or the WLS estimates of the parameters are employed. In particular, relative losses are about 0.12%, which is virtually the same value achieved also by estimating the parameters with the WLS approach over the whole dataset (namely including also the curves collected under partial shading). Hence, this clearly shows that the proposed WLS estimator is extremely robust with respect to a dataset containing values that have been measured under partial shading conditions, and thus not in agreement with the hypothesis of the model. On the other hand, adopting the LS estimator may result in similar performance when it is employed in conjunction with a method that allows removing data points which have been measured under partial shadowing. The drawback is that it leads to increased computational complexity. Finally, it is worth highlighting that when the parameters are computed on the refined dataset with the WLS estimator, Fig. 9 shows higher efficiency at very low solar irradiance levels (beginning of the day). However, the impact is marginal and not noticeable as long as the overall energy production during a day is considered.

4.2. Impact of database collection

As highlighted in Section 2.2, the most straightforward way to build the dataset that is required for estimating the parameters of the MB-MPPT algorithm is collecting a proper amount of volt-ampere curves of the module under different operating conditions, together with the corresponding

temperature. MPP voltage and current values can be easily extracted from the curves. The straightforward drawback is that energy production is not possible when curves are measured. Furthermore, measuring and processing the curves increases hardware requirements.

For this reason, it is extremely interesting to evaluate the performance achieved if the database is collected by executing a MPPT which does not requires a knowledge base, and by periodically saving the operating points. In this way, electricity is effectively produced also as long as the training set is built, thus increasing overall efficiency.

A P&O MPPT is considered for the purpose: similarly to the MB-MPPT, the algorithm operation is emulated using experimental data. In particular, the 10 curves in each block have been considered as the panel characteristics in 10 execution steps of the P&O algorithm, thus running with 100 ms sampling time (that is a typical value in practical implementations). The module voltage and current reached in the last characteristics of each block are stored in the database as estimate of MPP voltage and current, respectively. For each block, the initial panel voltage is supposed to be that reached at the end of the previous one. This permits obtaining another identification dataset having the same size as that used before.

Selecting the amplitude of the voltage perturbation ΔV has key importance for P&O algorithms, and in this case it also affects the quality of the training dataset. A smaller step clearly results in better accuracy under steady-state conditions. The MPP voltage values stored in the new database can be considered as corrupted by a zero-mean noise, whose magnitude corresponds to ΔV. However it is worth highlighting that a small value of ΔV leads to a slower tracking. Under rapidly changing conditions, slow dynamics means that the database may include a significant number of voltage and current measurements which are not in the neighborhood of the actual MPP. In order to avoid this situation, coarse values of perturbation step have been employed: 2.5% of V_{oc} and 1% of V_{oc}.

Considering these two values of ΔV, two different training datasets have been obtained. Parameters of the MB-MPPT have been estimated with both the LS and WLS approach, and the obtained results are reported in TABLE III.

TABLE III
ESTIMATED PARAMETERS, TRAINING DATA OBTAINED BY RUNNING A P&O MPPT ALGORITHM WITH TWO DIFFERENT VALUES OF PERTURBATION STEP

$\Delta V/V_{oc}$	Estimator	A_0 [V]	A_1 [V K^{-1}]	A_2 [V]	A_3 [V]
1%	LS	35.999	-0.0589	-1.28	-0.947
	WLS	37.146	-0.114	-0.705	-1.28
2.5%	LS	35.864	-0.0421	-1.36	-1.04
	WLS	36.930	-0.0930	-0.681	-1.45

From the previous table it appears that the values of the parameters obtained using the same estimator but the two different datasets which have been built by running the P&O MPPT are rather close to each other. Conversely, differences between LS and WLS estimates are much more significant in this respect. As explained before, the perturbation step introduces disturbances in both the MPP current and voltage values in the training database. MPP currents appear in the matrix **F** as arguments of logarithmic functions; therefore, the disturbance is expected to have rather small impact on **F**. As aforementioned, the voltage perturbation step can be modeled as additive uniform independent noise which is superimposed to the actual value of the vector $\mathbf{V}_{MP}$. However, it is reasonable that it has a slight impact on the parameter values, since the LS estimator is robust with respect to zero mean, independent additive noise. Therefore, it is not surprising that parameter values are rather close with respect to those reported in TABLE I, thus computed using the training database obtained from the *V-I* curves. Hence, good results are expected when these new parameter values are used in the MB-MPPT algorithm.

First of all, it is interesting to compare the panel voltages reached by the MB-MPPT employing all the different parameter estimates (database obtained from the *V-I* characteristics or from the P&O MPPT algorithm, LS and WLS estimators) with the actual MPPT voltage. Results are shown in Fig. 10 starting from about 9 am, in order not to show operation under severe partial shadowing.

Using the P&O MPPT algorithm in order to build the training set does not significant degrade achieved performance. In particular, when considering the smaller voltage step, the module voltages are extremely close to those reached as long as the identification database has been obtained from the *V-I* curves.

When comparing the LS and WLS estimates, the

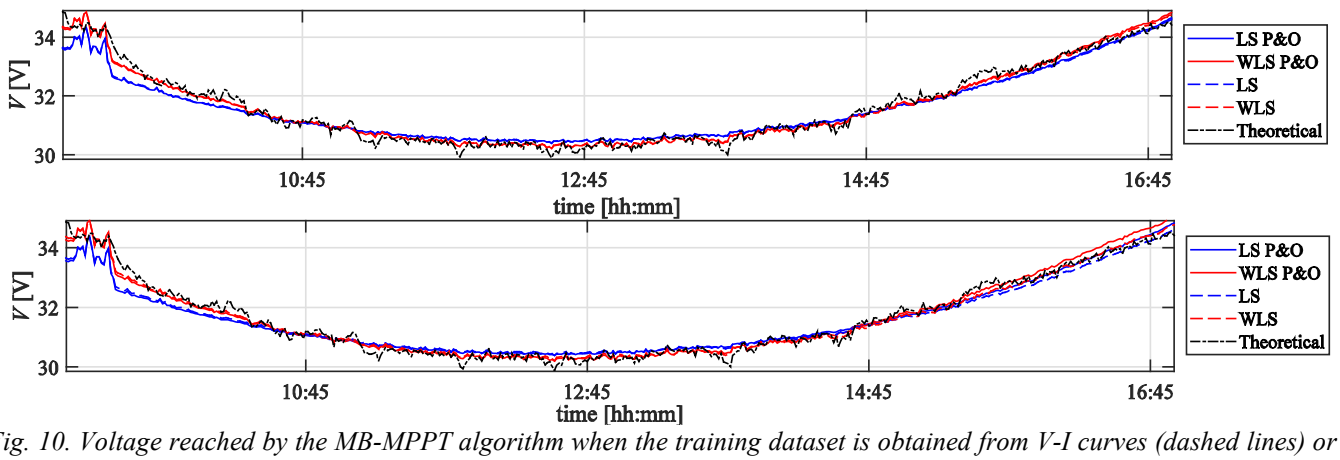

Fig. 10. Voltage reached by the MB-MPPT algorithm when the training dataset is obtained from V-I curves (dashed lines) or by running a P&O MPPT (continuous lines). $\Delta V/V_{oc}$=1% (upper graph) and $\Delta V/V_{oc}$ =2.5% (lower graph)

considerations carried out in the previous case still hold true: using the WLS approach to compute the parameters allows a more accurate MPP voltage tracking, in particular at the beginning and during the central part of the day. LS and WLS parameter estimations lead to virtually the same accuracy in the rightmost part of the graph.

Furthermore, the cumulative energy loss in relative value ($\Delta E_{e,r}$) defined as in (19) has been computed for all the different cases; Fig. 11 and Fig. 12 show results when the P&O step is respectively $\Delta V/V_{oc} = 1\%$ and $\Delta V/V_{oc} = 2.5\%$.

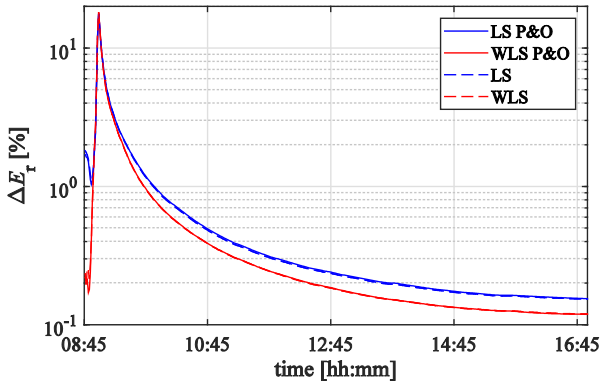

Fig. 11. Relative cumulative energy loss for LS and WLS parameter estimates, $\Delta V/V_{oc} = 1\%$

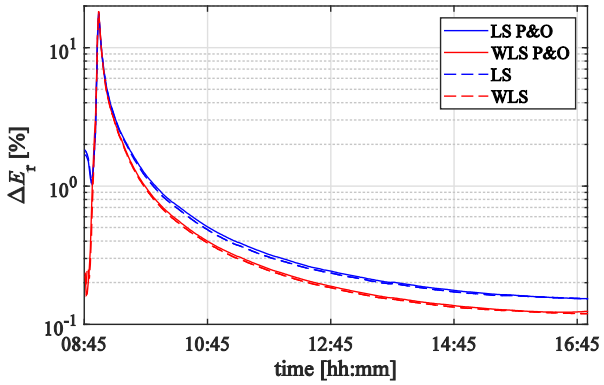

Fig. 12. Relative cumulative energy loss for LS and WLS parameter estimates, $\Delta V/V_{oc} = 2.5\%$

Both figures clearly indicate that using the P&O MPPT algorithm to build the training dataset instead of measuring the *V-I* curves have negligible impact on achieved efficiency. Moreover, it is interesting to highlight that also a rough perturbation step still provides remarkable results, thus highlighting the robustness of the estimates.

Finally, the cumulative energy loss ΔE defined as in (18) has been computed for the MB-MPPT algorithm using all the considered parameter estimates. Results after 9 am are summarized in Fig. 13. The figure highlights the higher efficiency reached by the MB-MPPT algorithm as long as the WLS estimates are employed: energy loss is always well below that obtained using the LS parameters estimations. At the end of the day, loss is 1.05 Wh with respect to 1.33 Wh (which is 27% higher) for a daily energy production of 868.3 Wh. This denotes the key importance of the method which is adopted to estimate the parameters in order to guarantee the best performance. Conversely, efficiency barely changes if the training dataset is built running a P&O MPPT or by measuring the *V-I* characteristics. However, the first choice have several advantages such as enabling energy production even during the training stage and opening the way to an adaptive update of the parameters in order to follow drift and degradation of the module.

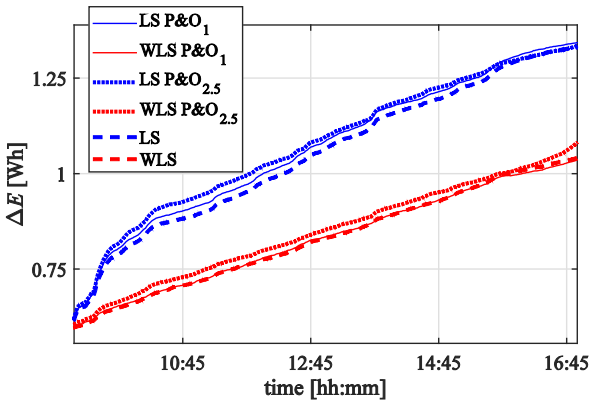

Fig. 13.Cumulative energy loss

5. Conclusion

This work deals with the performance optimization of a previously developed iterative MB-MPPT, which can be favorably exploited for module-level DMPPT. It enables good steady-state efficiency and fast tracking, but results strictly depend on the parameters of the underlying model. These parameters have to be estimated by collecting proper identification data before the MB-MPPT is put in operation; electricity generation is not generally possible during this stage, since it requires measuring volt-ampere characteristics of the module under different conditions. When the training database contains data measured under partial shadowing, the efficiency of the MB-MPPT algorithm is significantly reduced. However, the impact can be heavily mitigated by estimating the parameters with a proper WLS approach, as shown in this work. Furthermore, identification data can be produced also by running a simple P&O algorithm with a coarse perturbation step. In this way, energy is delivered to the grid even as long as the training database is built; experimental results show that there are no noticeable drawbacks in terms of achieved performance when the parameters of the MB-MPPT are estimated from this data. Finally, it may open the way to an adaptive update of the parameters of the MB-MPPT algorithm in order to achieve best performance even in case of drift, aging and degradation of the PV module.

6. References

[1] 'iea-pvps.org – Snapshot of Global PV Markets 2020' [Online]. Available at http://www.iea-pvps.org/index.php?id=266, accessed 24 April 2020

[2] 'Europe set to break solar records in 2020 says Solargis' [Online] https://www.smart-energy.com/renewable-energy/europe-set-to-break-solar-records-in-2020-says-solargis/, accessed 19 May 2020

[3] 'Smog-Free Skies Allow Germany to Break Record for Solar Power' [Online] https://www.bloombergquint.com/business/smog-free-skies-allow-germany-to-break-record-for-solar-power, accessed 19 May 2020

[4] Goodrich, A., James, T., Woodhouse, M.: 'Residential, commercial, and utility scale photovoltaic (PV) system prices in the United States: current drivers and cost-reduction opportunities', Technical Report TP-6A20-53347, NREL, Golden, CO, 2012
[5] Pyrgou, A., Kylili, A., Fokaides, P. A.: 'The future of the Feed-in Tariff (FiT) scheme in Europe: The case of photovoltaics', *Energy Policy*, 2016, **95**, pp. 94-102
[6] Femia, N., Petrone, G., Spagnuolo, G., Vitelli, M.: 'Optimization of perturb and observe maximum power point tracking method', *IEEE Trans. Power Electron.*, 2005, **20**, (4), pp. 963-973
[7] Kish, G. J, Lee, J. J., Lehn, P. W.: 'Modelling and control of photovoltaic panels utilising the incremental conductance method for maximum power point tracking' *IET Renew. Power Gener.*, 2012, **6**, (4), pp. 259-266
[8] Sera, D., Mathe, L., Kerekes, T., Spataru, S. V., Teodorescu, R.: 'On the perturb-and-observe and incremental conductance MPPT methods for PV Systems', *IEEE J. Photovolt.*, 2013, **3**, (3), pp. 1070-1078
[9] Piegari, L., Rizzo, R.: 'Adaptive perturb and observe algorithm for photovoltaic maximum power point tracking', *IET Renew. Power Gener.*, 2010, 4, (4), pp. 317–328
[10] Liu, F., Duan, S., Liu, F., Liu, B. Kang, Y.: 'A variable step size INC MPPT method for PV systems', *IEEE Trans. Ind. Electron.*, 2008, **55**, (7), pp. 2622-2628
[11] Rezk, H., Eltamaly, A. M.: 'A comprehensive comparison of different MPPT techniques for photovoltaic systems', *Solar Energy*, 2015, **112**, pp. 1-11
[12] Podder, A. K., Roy, N. K., Pota, H. R.: 'MPPT methods for solar PV systems: a critical review based on tracking nature' *IET Renew. Power Gener.*, 2019, **13**, pp. 1615-1632
[13] Subudhi, B., Pradhan, R.: 'A comparative study on maximum power point tracking techniques for photovoltaic power systems', *IEEE Trans. Sustain. Energy*, 2013, **4**, (1), pp. 89-98
[14] Karami, N., Moubayed, N., Outbib, R.: 'General review and classification of different MPPT Techniques', *Renewable and Sustainable Energy Reviews*, 2017, **68**, pp. 1-18
[15] Costabeber, M., Carraro, M., Zigliotto, M.: 'Convergence analysis and tuning of a sliding-mode ripple-correlation MPPT', *IEEE Trans. Energy Convers.*, 2015, **30**, (2), pp. 696-706
[16] Belkaid, A., Gaubert, J., Gherbi, A.: 'Design and implementation of a high-performance technique for tracking PV peak power', *IET Renew. Power Gener.*, 2017, **11**, (1), pp. 92-99
[17] Mohd Zainuri, M. A. A., Mohd Radzi, M. A., Soh, A. C., Rahim, N. A.: 'Development of adaptive perturb and observe-fuzzy control maximum power point tracking for photovoltaic boost dc-dc converter', *IET Renew. Power Gener.*, 2014, **8**, (2), pp. 183-194
[18] Kottas, T. L., Boutalis, Y. S., Karlis, A. D.: 'New maximum power point tracker for PV arrays using fuzzy controller in close cooperation with fuzzy cognitive networks', *IEEE Trans. Energy Convers.*, 2006, **21**, (3), pp. 793-803
[19] Metry, M., Shadmand, M. B., Balog, R. S., Abu-Rub, H.: 'MPPT of photovoltaic systems using sensorless current-based model predictive control', *IEEE Trans. Ind. Appl.*, 2017, **53**, (2), pp. 1157-1167
[20] Elobaid, L. M., Abdelsalam, A. K., Zakzouk, E. E.: 'Artificial neural network-based photovoltaic maximum power point tracking techniques: a survey', *IET Renew. Power Gener.*, 2015, **9**, (8), pp. 1043-1063
[21] Petrone, G., Spagnuolo, G., Teodorescu, R., Veerachary M., Vitelli, M.: 'Reliability issues in photovoltaic power processing systems', *IEEE Trans. Ind. Electron.*, 2008, **55**, (7), pp. 2569-2580
[22] Dhimish, M.: 'Assessing MPPT Techniques on hot-spotted and partially shaded photovoltaic modules: comprehensive review based on experimental data', *IEEE Trans. Electron Devices*, 2019, **66,** pp. 1132-1144
[23] Carannante, G., Fraddanno, C., Pagano, M., Piegari, L.: 'Experimental performance of MPPT algorithm for photovoltaic sources subject to inhomogeneous insolation', *IEEE Trans. Ind. Electron.*, 2009, **56**, (11), pp. 4374-4380
[24] Liu, Y., Huang, S., Huang J., Liang, W.: 'A particle swarm optimization-based maximum power point tracking algorithm for PV systems operating under partially shaded conditions', *IEEE Trans. Energy Convers.*, 2012, **27**, (4), pp. 1027-1035
[25] Ramyar, A., Iman-Eini, H., Farhangi, S.: 'Global maximum power point tracking method for photovoltaic arrays under partial shading conditions', *IEEE Trans. Ind. Electron.*, 2017, **64**, (4), pp. 2855-2864
[26] MacAlpine, S. M., Erickson, R. W., Brandemuehl, M. J.: 'Characterization of power optimizer potential to increase energy capture in photovoltaic systems operating under nonuniform conditions', *IEEE Trans. Power Electron.*, 2013, **28**, (6), pp. 2936-2945
[27] Bastidas-Rodriguez, J. D., Franco, E., Petrone, G., Ramos-Paja, C. A., Spagnuolo, G.: 'Maximum power point tracking architectures for photovoltaic systems in mismatching conditions: a review' *IET Power Electron.*, 2014, **7**, (6), pp. 1396-1413
[28] Farh, H. M. H., Eltamaly A. M., Al-Saud, M. S.: 'Interleaved boost converter for global maximum power extraction from the photovoltaic system under partial shading', *IET Renew. Power Gener.*, 2019, **13**, (8), pp. 1232-1238
[29] Hasan, R., Hassan, W., Farhangi, M., Mekhilef, S. Xiao, W.: 'Enhanced soft-switching strategy for flyback-based microinverter in PV power systems', *IET Renew. Power Gener.*, 2019, **13**, (15), pp. 2830-2839
[30] Chiu, H. *et al.*: 'A module-integrated isolated solar microinverter', *IEEE Trans. Ind. Electron.*, 2013, **60**, (2), pp. 781-788
[31] Kwon, J.-M., Kwon, B.-H, Nam, K.-H, 'High-efficiency module-integrated photovoltaic power conditioning system', *IET Power Electron.*, 2009, **2**, (4), pp. 410-420
[32] Kasper, M., Bortis, D., Kolar, J. W.: 'Classification and comparative evaluation of PV panel-integrated DC–DC converter concepts' *IEEE Trans. Power Electron.*, 2014, **29**, (5), pp. 2511-2526
[33] Hua, C., Fang, Y., Wong, C.: 'Improved solar system with maximum power point tracking', *IET Renew. Power Gener.*, 2018, **12**, (7), pp. 806-814
[34] Leuenberger, D., Biela, J.: 'PV-module-integrated AC inverters (AC modules) with subpanel MPP tracking', *IEEE Trans. Power Electron.*, 2017, **32**, (8), pp. 6105-6118
[35] Rahman, S. A., Varma, R. K., Vanderheide, T.: 'Generalised model of a photovoltaic panel', *IET Renew. Power Gener.*, 2014, **8**, (3), pp. 217-229
[36] Cristaldi, L., Faifer, M., Rossi, M., Toscani, S.: 'A simplified model of photovoltaic panel', *Proc. IEEE Int. Instrumentation and Measurement Technology Conf.*, 2012, pp. 431-436
[37] Lasheen, M., Abdel Rahman, A. K., Abdel-Salam, M., Ookawara, S.: 'Adaptive reference voltage-based MPPT technique for PV applications', *IET Renew. Power Gener.*, 2017, **11**, (5), pp. 715-722
[38] Miao, J., Xie, D., Fan, R.: 'One-step MPPT method based on five-parameter model of PV panel', *The Journal of Engineering*, 2017, (13), pp. 917-921
[39] Vicente, E. M., dos Santos Vicente, P., Moreno, R. L., Ribeiro, E. R.: 'High-efficiency MPPT method based on irradiance and temperature measurements', *IET Renew. Power Gener.*, 2020, **14**, no. 6, pp. 986-995, 27 4 2020.
[40] Cristaldi, L., Faifer, M., Rossi, M., Toscani, S.: 'MPPT definition and validation: a new model-based approach', *Proc. IEEE Int. Instrumentation and Measurement Technology Conf.*, 2012, pp. 594-599

[41] Cristaldi, L., Faifer, M., Rossi, M., Toscani, S.: 'An improved model-based maximum power point tracker for photovoltaic panels', *IEEE Trans. Instrum. Meas.*, 2014, **63**, (1), pp. 63-72
[42] Faifer, M., Cristaldi, L., Toscani, S., Soulantiantork, P., Rossi, M.: 'Iterative model-based maximum power point tracker for photovoltaic panels', *Proc. IEEE Instrumentation and Measurement Technology Conf.*, 2015, pp. 1273-1278.
[43] Soulatiantork, P., Cristaldi, L., Faifer, M., Laurano, C., Ottoboni, R., Toscani, S.: 'A tool for performance evaluation of MPPT algorithms for photovoltaic systems' *Measurement*, 2018, **128**, pp. 537-544
[44] Cristaldi, L., Faifer, M., Laurano, C., Ottoboni, R., Toscani, S., Zanoni, M.: 'Model-based MPPT parameter optimization for photovoltaic panels', *Proc. Int. Conf. on Clean Electrical Power*, 2019, pp. 534-538
[45] Luque, A., Hegedus, S.: 'Handbook of photovoltaic science and engineering', 2010, 2nd ed., New York: John Wiley & Sons